Model Interpretation of Non-Dipolar Integral Body Surface QRST Maps Randomly Appearing in Arrhythmia Patients

G. Kozmann*, Z. Tarjányi*, G. Tuboly*,
V. Szathmáry, J. Svehlikova***, M. Tysler*****

**Faculty of Information Technology, University of Pannonia, Veszprem, Hungary,*
(e-mail: kozmann@irt.vein.hu)
***Institute of Normal and Pathological Physiology, SAS, Bratislava, Slovakia,*
(e-mail: vszathmary@chello.sk)
****Institute of Measurement Science, SAS, Bratislava, Slovakia,*
(e-mail:umertysl@savba.sk)

Abstract: The source level interpretation of beat-to-beat QRST integral map non-dipolarity index (NDI) fluctuation has been studied, with a special regard to the generation of extremely large amplitude spikes. Computations relied on a numerical heart and chest model with modifiable action potential (AP) patterns, as well as ectopic activation wave generation possibility. These features are suitable for quantitative modeling of ventricular heterogeneity which is a prerequisite of malignant arrhythmias. According to the results skewed NDI distributions were generated by AP modulation, but extreme NDIs occurred due to apical ectopic beats propagating from the epicardium towards the endocardium.

Keywords: ***Non-dipolarity index, numerical chest model, numerical heart model, NDI spikes***

1. INTRODUCTION

Ventricular fibrillation is the most common cause of sudden cardiac death (SCD). According to experimental and theoretical studies the biophysical substrate of ventricular fibrillation is connected to the structural and/or dynamical repolarization dispersion (RD) changes, Kléber and Rudy (2004). According to a recent scientific statement of the AHA/ACCF/HRS, current non-invasive risk assessment methods are not efficient enough; further efforts are justified for their improvement, Goldberger et al. (2008). In our long term pursuit for an improved non-invasive SCD risk assessment, we used QRST body surface potential maps instead of conventional ECG leads, in order to grasp the whole RD related information accessible on the thoracic surface, Kozmann et al. (2010). A simplified arrhythmia vulnerability index based on the QRST integral of the Frank leads was recently suggested by Tereshchenko et al. (2010 and 2011). The theoretical basis of our QRST integral map-based RD detection was proved precisely by Geselowitz (1983). The novelty in our approach was essentially the beat-to-beat QRST integral map analysis to reveal both spatial and temporal RD irregularities after the pioneering work of Abildskov et al. (1982), Berger et al. (1997), and Atiga et al. (1998). A different risk assessment approach based on high-resolution body surface potential maps has been published recently by Fereniec at al. (2011).

Due to the spatial filtering effect of the body as a volume conductor, RD, on the epicardial surface generally result in a "dipolar pattern" on the thoracic surface by visual inspection (i.e. one convex positive and one negative region) on the chest surface. However, non-dipolarity indices (NDI), computed from the coefficients of Karhunen-Loeve (KL) expansion of the QRST integral maps characterize sensitively the spatio-temporal variability of the subsequent QRST integral maps, Lux et al. (1981). In our small-sample study, beat-to-beat NDI plots sensitively illustrated the significant changes of RD in the group of implanted cardioverter (ICD) patients with documented malignant arrhythmia vulnerability, Kozmann et al. (2010). In statistical terms NDI histograms showed skewed lognormal distributions, sometime with NDI values up to 0.9, while in normal subjects the subsequent NDI values remained typically in the range of 0.1-0.2.

In this study we attempted to give a source level explanation of the observed normal and pathological NDI behaviour, with a special regard to the extremely large NDI spikes. To this end, numerical chest and heart models were used.

2. MATERIALS AND METHODS

2.1 Model of cardiac ventricles

Details of our computer model of human cardiac ventricles were described previously, Szathmáry and Osvald (1994). Briefly, the model is defined in a 3-dimensional matrix of cubic elements, where these elements represent the functional property of an excitable cardiac tissue and ventricular transmembrane action potentials (MoAPs). The geometry of cardiac ventricles is defined analytically by parts of ellipsoids representing their inner (endocardial) and outer (epicardial) surfaces. Characteristics of these ellipsoids are derived from the gross dimensions of the right (RV) and left (LV) ventricle and from the thicknesses of their walls, given as the input data of the required model. To simulate the repolarization

heterogeneity, ventricular walls are sliced to 5 layers, paralleling with their inner and outer surfaces (Fig. 1). The characteristics of model elements may be defined differently in dependence on their localization in respective layers, (Fig. 1), Szathmáry and Ruttkay-Nedecký (2002).

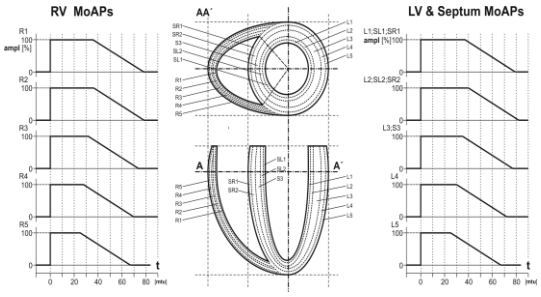

Fig. 1. A schematic representation of left and right ventricular heart geometry of the healthy heart, with the simplified reference model action potentials (MoAPs).

For the presented reference model, simulating the normal activation of human ventricles, the gross dimensions of ventricles and the parameters of activation, were derived from published data, Hutchins et al. (1978), Durrer et al. (1970). The ventricular depolarization was started from predetermined elements on the inner - endocardial surface of both ventricles, corresponding to regions of earliest activation. The spread of activation in the inner layers, representing the Purkinje mesh, was three times faster than in the remaining layers of the walls. After depolarizing of a model elements their consecutive repolarization is governed by their MoAPs. These MoAPs in respective layers reflect the transmural dispersion of cardiac action potential durations. The activation of the reference model, defined in this way corresponded well with generally accepted normal patterns of human heart activation.

The model allows simulation of regions in the ventricular wall with distinct repolarization patterns with respect to the remaining parts of the ventricle (Fig. 2). Furthermore, additional activation points (ectopic activation) are possible in arbitrary points of the myocardium. Their locations and shapes are defined also analytically by subsidiary ellipsoids (i.e.: Fig. 3).

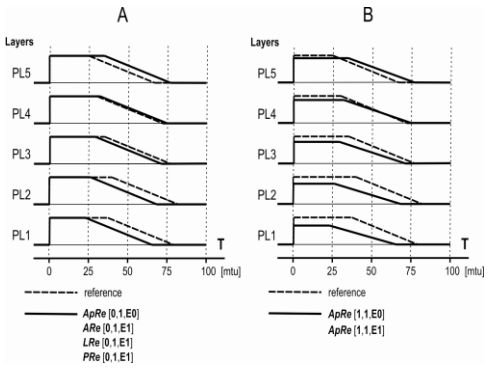

Fig. 2. Possible pathologic modulation of MoAPs in our modelling study.

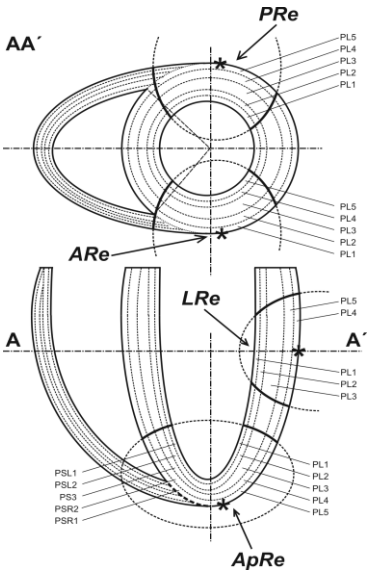

Fig. 3. Location of epicardial ectopic foci in our modeling of extreme NDIs.

The spread of activation wavefront was simulated by cellular automaton. In each step of simulation the elementary dipole moments were computed as the potential difference between the adjacent elements. Finally, the whole model of the cardiac ventricles' myocardium was divided into 33 volume segments. In each segment the dipole moments from all corresponding elements were summarized in its gravity centre, so that the multiple dipole equivalent cardiac generators were created (Fig. 4).

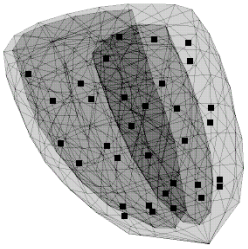

Fig. 4. The model of analytically defined myocardium of the left and right ventricle. Black points indicate the positions of dipoles of the multiple-dipole equivalent generator.

2.2 Simulation of body surface potential maps (BSPMs)

To compute the electrocardiological potentials on the surface of human thorax, the multiple dipole model of the cardiac generator was inserted in a realistically shaped torso model (Fig. 5). Models of lungs with 4x lower conductivity than general conductivity of the torso and ventricular cavities with 3x higher conductivity were inserted in torso introducing (assuming) main inhomogeneities. The electric potentials on the body surface were computed in the points of the torso model using boundary element method (BEM), which was proposed already in Barr et al. (1966) and is frequently used up to this day, Tyšler et al. (2005).

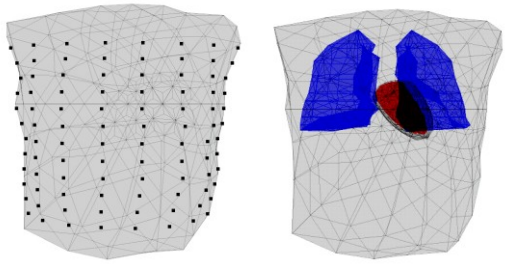

Fig. 5. Left: The realistically shaped torso model with black points indicating the frontal position of nodes in regular mesh, in which the BSPM is computed. Right: The inhomogeneous torso model configuration for simulations of BSPMs from modelled cardiac generator.

The use of BEM for computation of body surface potential maps $m(t)$ in Ne points on the body surface in each time instant t yields a linear matrix equation:

$$m(t) = A\, g(t) \tag{1}$$

where A is the time independent transfer matrix, which represents the properties of inhomogeneous torso as the volume conductor and $g(t)$ is multiple dipole generator (with Ns dipoles) in particular time step of the heart activation. The integral BSPM p representing the integral of $m(t)$ over particular time interval could be then described by (2).

$$p = \int m(t)dt = \int A\, g(t)dt = A\int g(t)dt = A\, s \tag{2}$$

Where s represents the time integrals of Ns dipole moments of modelled multiple current dipoles' generator. Considering three orthogonal components of each dipole moment the size of the transfer matrix A is (Ne x $3Ns$).

The body surface potential maps were computed from the potentials in regular mesh (12 x 16) on the body surface consisted from 192 points (Fig. 5).

2.3 Simulated changes of ventricular activation

The aim of simulated changes of the modeled cardiac generator was to obtain integral BSPM with pattern and non-dipolarity index similar to that randomly occurred integral BSPM in the measured arrhythmia patient.

Under pathological circumstances the MoAP amplitude and/or duration was modulated in some segments of the ventricular wall. In Fig. 3 MoAPs were altered in segments shown at the apex and at mid-anterior, mid-lateral and mid-posterior part of the ventricular model as a consequence of ectopic beats starting simultaneously with the beginning of the normal ventricular activation onset. The locations are represented on the epicardium by the asterisks. Due to the epicardial focus of the ectopic beats we supposed that MoAPs duration is gradually decreasing from the epicardium to the endocardium. In the modeling experiment the four types of ectopic beats were generated subsequently, not simultaneously.

Changes of the length and/or the shape of APs influence the amplitude of QRST integrals at an arbitrary body surface point P. Consequently, beat-to-beat application of (3) provides a noninvasive tool that can be used to study the spatio-temporal properties of RD.

$$\int_{QRST} \phi(P,t)dt = -k\iiint_{V_s} \mathbf{z}(P,\mathbf{r})\nabla\mu(\mathbf{r})dV_s \tag{3}$$

where:

$$\mu = \int_{QRST} [\phi_m(\mathbf{r},t) - \phi_{mr}(\mathbf{r})]dt \qquad \text{(i.e.: area of MoAP)} \tag{4}$$

$\phi_m(\mathbf{r},t)$: membrane potential at time t
$\phi_{mr}(\mathbf{r})$: membrane resting potential at point $\mathbf{r}$
V_s: volume of sources (myocardium)
k: constant
z: vector of transfer coefficients between P and $\mathbf{r}$

QRST integral maps were characterized by the beat-to-beat sequence of non-dipolarity indices (NDI).

$$NDI = \frac{\sum_{i=4}^{12} c_i^2}{\sum_{i=1}^{12} c_i^2} = \frac{P_{ND}}{P_D + P_{ND}} \cdot 100\% \tag{5}$$

Where:

P_D: BSPM signal power represented by the "dipolar" KL components (i: 1-3) according to Lux et al (1981)
P_{ND}: BSPM signal power represented by the "non-dipolar" KL components (i: 4-12) according to Lux et al (1981)

3. RESULTS AND DISCUSSION

NDI values obtained by the normal activation sequence and by the four "ectopic beats" generating an opposite activation front to the normal spread of activation with altered MoAPs duration within the elliptical areas shown in Fig. 3 are listed in Table 1.

Table 1 Selected results of NDI simulations in physiological case with four epicardial ectopic activations

Model	NDI(QRST) %
Reference	12.1
ApRe	91.6
ARe	7.8
LRe	8.6
PRe	6.2

Explanations: ApRe - apical, ARe - anterior, LRe - lateral, PRe – posterior regions of distinct repolarization.

A systematic exploration of MoAP modulation effects on the NDI values revealed that the NDI spikes frequently observed in ICD patients can be generated in our conceptual model by apical extra activation fronts spreading from the epicardium to the endocardium. According to our assumption, the MoAP duration in this case is the largest in the firstly activated epicardial layer, gradually decreasing in the subepicardial layers, i.e. the physiological MoAP duration decreasing from the endocardium to the epicardium is reversed. (We should remark, that the reversed MoAP duration at the apex might be a result of a changed intra- and extracellular level regulation of the ionic transport.) In the time domain the above "ectopic beat" is initiated simultaneously with the initiation of the ventricular activation. However, similar epicardial-to-endocardial ectopic beats on the mid-anterior, mid-lateral and mid-posterior regions do not result in high NDI amplitude spikes (see Table 1), probably due to the early collision of these additional waves with the activation waves originating physiologically from the endocardium.

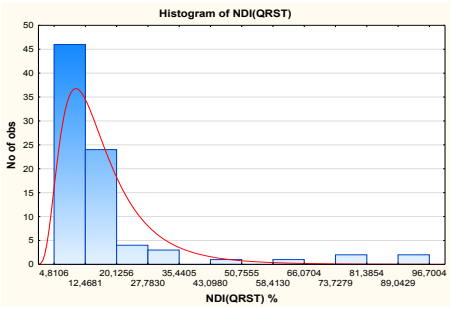

Fig. 6. NDI histogram of 100 subsequent simulated beats with ventricular heterogeneity. The histogram was approximated by lognormal distribution exactly as it was in the case of the NDI histogram of an ICD patient shown in Fig. 7.

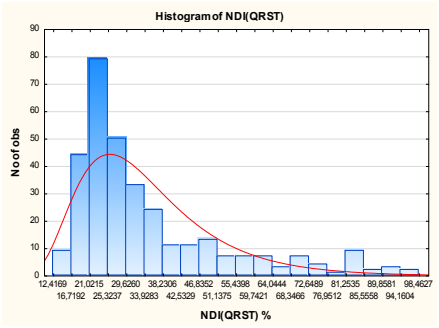

Fig. 7. NDI histogram of an arrhythmia patient with implanted cardioverter defibrillator (ICD).

The local perturbation of MoAP parameters (amplitude and/or duration) increases the variability of NDI values, approximately according to the lognormal distribution. The lognormal character of the NDI distribution is a consequence of the asymmetric position of the heart within the thorax.

Fig. 8 shows experimental data obtained in an ICD patient before and at the time of an NDI spike.

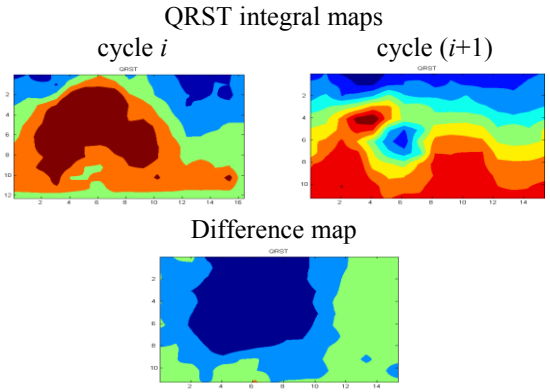

Fig. 8. Subsequent rolled-out QRST integral maps of an ICD patient, and their difference. (In all the maps the left side of the map shows the frontal side of the torso, the right side shows the back. The upper border is in the height of the clavicular notch, the lower one at the umbilicus.) The RR interval and QRS width was normal in these beats. Cycle *i* belongs to a normal beat with low NDI, while *i*+1 to a cycle with high NDI. In the latter case the integral map distribution is clearly non-dipolar. The difference map suggests a superimposed waveform originating from an activation wave spreading from the epicardium towards the endocardium.

The generation of NDI spikes in the sequence of cardiac cycles was explained in details by Kozmann et al. (2010). The necessary condition of extremely elevated NDIs was related to the high standard deviation values of "dipolar KL components" compared with the "mean dipolar components". The frequency of the elevated NDIs demonstrated by their skewed (lognormal) distribution is a marker of the increased arrhythmia vulnerability.

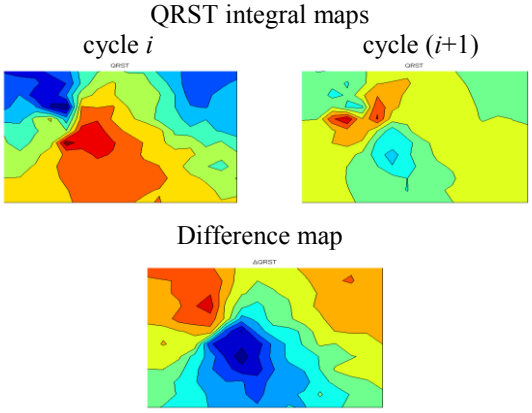

Fig. 9. Computer simulation of QRST integral maps of two subsequent cardiac cycles. The first one represents a normal beat, while in the second one an epicardial ectopic wavefront was launched from the apical area. In the second QRST integral map the resultant non-dipolar pattern is clearly visible. The difference of the subsequent QRST integrals (due to the superimposed ectopic beat) is essentially dipolar (as it was in Fig. 8 as well).

According to Tereshchenko et al (2011), the sum magnitude of Frank-lead QRST integral is a promising new marker of ventricular tachycardia risk. Essentially this marker is related to the significantly decreased dipolar components, i.e., this conclusion is compatible with our findings. Fereniec et al. (2011) limited the analysis only to the averaged body surface potential map cycle. Though their discriminative parameters have no direct physical meaning, they characterize the essential signal properties of the ST segment as well as the relationship of the cardiac depolarization and repolarization implicitly supporting our results.

ACKNOWLEDGEMENT

This study was supported by grants TÁMOP-4.2.2-08/1/2008-0018 and TÁMOP-4.2.2/B-10/1-2010-0025 projects, Hungary, and by the Slovak Research and Development Agency No. APVV-0513-10.

REFERENCES

Abildskov, J.A., Green, L.S., Evans, A.K., and Lux, R.L. (1982). The QRST deflection area of electrograms during global alterations of ventricular repolarization. *J. Electrocardiol.*, 15 (2), 103-107.

Atiga, W.L., Calkins, H., Lawrence, J.H., Tomaselli, G.F., Smith, J.M., and Berger, R.D. (1998). Beat-to-beat repolarization lability identifies patients at risk for sudden cardiac death. *J. Cardiovasc. Electrophysiol.*, 9 (9), 899-908.

Barr, R.C., Pilkington, T.C., Boineau, J.P., and Spach, M.S. (1966). Determining Surface Potentials from Current Dipoles, with Application to Electrocardiography. *IEEE Transactions on Biomedical Engineering*, 13, 88-92.

Berger, R.D., Kasper, E.K., Baughman, K.L., Marban, E., Calkins, H., and Tomaselli, G.F. (1997). Beat-to-beat QT interval variability: novel evidence for repolarization lability in ischemic and nonischemic dilated cardiomyopathy. *Circulation*, 96 (5), 1557-1565.

Durrer, D., Van Dam, R.TH., Freud, G.E., Janse, M.J., Meijler, F.L., and Arzbaecher, R.C. (1970). Total excitation of the isolated human heart. *Circulation*, 41, 899-912.

Fereniec, M., Stix, G., Kania, M., Mroczka, T., Janusek, D., Maniewski, R. (2011). Risk assessment of ventricular arrhythmia using new parameters based on high resolution body surface potential mapping. *Med. Sci. Monit.*, 17 (3), 26-33.

Geselowitz, D.B. (1983). The ventricular gradient revisited: relation to the area under the action potential. *IEEE Trans. Biomed. Eng.*, 30 (1), 76-77.

Goldberger, J.J., Cain, M.E., Hohnloser, S.H., Kadish, A.H., Knight, B.P., Lauer, M.S., Maron, B.J., Page, R.L., Passman, R.S., Siscovick, D., Siscovick, D., Stevenson, W.G., and Zipes, D.P. (2008). American Heart Association/American College of Cardiology Foundation/Heart Rhythm Society Scientific Statement on Noninvasive Risk Stratification Techniques for Identifying Patients at Risk for Sudden Cardiac Death: A scientific statement from the American Heart Association Council on Clinical Cardiology Committee on Electrocardiography and Arrhythmias and Council on Epidemiology and Prevention. *Circulation*, 118 (14), 1497-1518.

Hutchins, G.M., Bulkley, B.H., Moore, G.W., Piasio, M.A., and Lohr, F.T. (1978). Shape of the human cardiac ventricles. *Am. J. Cardiol.*, 41, 646-654.

Kléber, A.G., and Rudy, Y. (2004). Basic mechanisms of cardiac impulse propagation and associated arrhythmias. *Physiol. Rev.*, 84 (2), 431-488.

Kozmann, G., Haraszti, K., and Préda, I. (2010). Beat-to-beat interplay of heart rate, ventricular depolarization, and repolarization. *J. Electrocardiol.*, 43 (1), 15-24.

Lux, R.L., Evans, A.K., Burgess, M.J., Wyatt, R.F., and Abildskov, J.A. (1981). Redundancy reduction for improved display and analysis of body surface potential maps. I. Spatial compression. *Circulation*, 49 (1), 186-196.

Stenroos, M. (2009). The transfer matrix for epicardial potential in a piece-wise homogeneous thorax model: the boundary element formulation. *Physics in Medicine and Biology*, 54, 5443-5455.

Szathmáry, V. (2006). Model based analysis of the cardiac electric field. In Pecháňová, O., and Jagla, F., (ed.), *Selected diseases of civilization – basic mechanisms and clinical implications*, 105-126. Comenius University, Bratislava.

Szathmáry, V., and Osvald, R. (1994). An interactive computer model of propagated activation with analytically defined geometry of ventricles. *Comput. Biomed. Res.*, 27, 27-38.

Szathmáry, V., and Ruttkay-Nedecký, I. (2002). Effect of different sources of ventricular repolarization heterogeneity on the resultant cardiac vectors. In Surján G., Engelbrecht, R., and McNair, P., (ed.), *Data in the Information Society*, 88-92. IOS Press, Amsterdam, Berlin, Oxford, Tokyo, Washington.

Tereshchenko, L.G., Cheng, A., Fetics, B.J., Marine, J.E., Spragg, D.D., Sinha, S., Calkins, H., Tomaselli, G.F., Berger, R.D. (2010). Ventricular arrhythmia is predicted by sum absolute QRST integral but not by QRS width. *J Electrocardiol.*, 43 (6), 548-552.

Tereshchenko, L.G., Cheng, A., Fetics, B.J., Butcher, B., Marine, J.E., Spragg, D.D., Sinha, S., Dalal, D., Calkins, H., Tomaselli, G.F., Berger, R.D. (2011). A new electrocardiogram marker to identify patients at low risk for ventricular tachyarrhythmias: sum magnitude of the absolute QRST integral. *J. Electrocardiol.*, 44 (2), 208-216.

Tyšler, M., Turzová, M., Tiňová, M., Švehlíková, J., Hebláková, E., Szathmáry, V., and Filipová, S. (2005). Use of body surface potential maps for model-based assessment of local pathological changes in the heart. *Bulletin of the Polish Academy of Sciences: Technical Sciences*, 53 (4), 207-215.